IEEE Photonics Journal
An IEEE Photonics Society Publication

Photonic-Assisted Microwave Frequency and Phase Shifter for Deception Jamming

Volume 13, Number 3, June 2021

Chongjia Huang
Erwin H. W. Chan, ***Senior Member, IEEE***

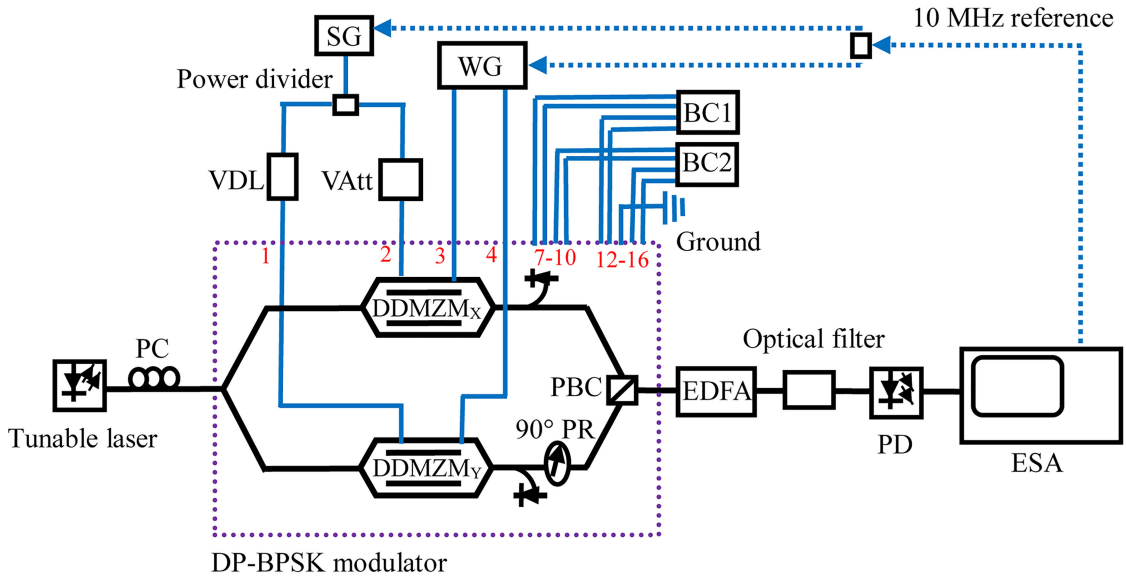

DOI: 10.1109/JPHOT.2021.3074164

Photonic-Assisted Microwave Frequency and Phase Shifter for Deception Jamming

Chongjia Huang and Erwin H. W. Chan, *Senior Member, IEEE*

College of Engineering, IT and Environment, Charles Darwin University, Darwin, NT 0909, Australia

DOI:10.1109/JPHOT.2021.3074164

Manuscript received March 26, 2021; accepted April 15, 2021. Date of publication April 20, 2021; date of current version April 29, 2021. Corresponding author: Erwin H. W. Chan (e-mail: erwin.chan@cdu.edu.au).

Abstract: A new microwave photonic signal processing structure that has the ability to realise frequency and phase shifting operation is presented. The proposed structure uses Serrodyne phase modulation in a dual-polarisation binary phase shift keying (DP-BPSK) dual-drive Mach Zehnder modulator to shift the frequency of an input microwave signal. This has the advantage over the conventional frequency mixers that the unwanted frequency components adjacent to the frequency translated microwave signal can be largely suppressed. It is suitable for use in deception jamming in electronic countermeasures systems. The phase shifting operation is realised by controlling the bias voltages of the DP-BPSK modulator. The dual-function microwave photonic signal processor has a simple structure and a wide bandwidth. The structure enables commercial modulator bias controllers to be used to provide long-term stable performance. Experimental results are presented that demonstrate a wide operating frequency range of 3 to 16 GHz, an over 35 dB suppression on the spurious signals and 0° to 360° phase shift on the frequency translated microwave signal. Using bias controllers to maintain a large spurious suppression ratio of around 35 dB is also demonstrated.

Index Terms: Optical signal processing, microwave frequency translation, optical modulators, Serrodyne modulation.

1. Introduction

Modern radar systems use the properties of the retuned radar signal to determine target information such as its velocity, distance and position. Various techniques have been developed to avoid a target being detected. One of them is called deception jamming. A deception jammer receives the radar signal, modifies the signal properties and transmits the modified signal back to the hostile radar. Since the velocity of a target can be obtained from the difference between the transmitted and returned radar signal frequencies, a frequency translator can be installed in the target to alter the radar signal frequency. This causes the radar, which receives the modified radar signal, to misidentify the target velocity. This is called velocity deception [1]. The phase of a radar signal also contains target information. For examples moving-target indication (MTI) radars use the returned radar signal phase to determine whether the target is a moving or stationary object [2] and synthetic-aperture radars use the returned radar signal phase for imaging [3]. Therefore, it is important to modify both the frequency and phase of a radar signal to provide false target information to the hostile radar for electronic countermeasures.

Considering the example given in [1] where a target is travelling with a velocity of 1829 m/s. This generates a 146 kHz Doppler frequency shift (DFS) for a microwave signal with a 12 GHz carrier frequency. Adding an additional $\pm$25 kHz to this frequency shifted microwave signal introduces around $\pm$304 m/s of uncertainty in the relative velocity of the target. This indicates that, for velocity deception, only a small change of less than 1 MHz in a radar signal frequency is needed. A frequency translator rather than a frequency mixer is used to accomplish this small frequency translation. This is because a conventional mixer generates unwanted frequency components, referred to as the spurious signals, in addition to the wanted frequency translated microwave signal. For example, using a mixer to shift the input microwave signal at the frequency of f_{RF} to $f_{RF} + f_s$ where f_s is the amount of frequency translation, the mixer output not only consists of a frequency translated microwave signal at $f_{RF} + f_s$ but also a carrier at f_{RF} and a sideband at f_{RF}-f_s. Since the amount of frequency translation is less than 1 MHz, these spurious signals are located inside the frequency translated microwave signal bandwidth. A microwave filter cannot be used to remove these spurious signals.

Processing radar signals using microwave photonic techniques has the benefits of wide bandwidth, immunity to electromagnetic interference, reconfigurability, and parallel and multiple signal processing capabilities, compared to conventional electronic approaches. Many microwave photonic signal processing structures for simultaneously realising frequency mixing and phase shifting operations have been reported [4]–[7]. However, they are not suitable for frequency translation due to spurious signals generated at the output as was discussed in the previous paragraph. A frequency translator implemented by Serrodyne phase modulation can generate a clean frequency translated microwave signal. There are few reports on microwave photonic frequency translators [8]–[10]. The early reported microwave photonic frequency translator [8] consists of two laser sources, two separated Mach Zehnder modulators (MZMs), an optical coupler and a photodetector. It is based on applying a sawtooth wave to a microwave photonic phase shifter to shift the microwave signal frequency. It has the same operating principle as the electronic frequency translators [11], [12]. This reported microwave photonic frequency translator has a number of drawbacks. First, the two path lengths between the MZMs and the photodetector need to be matched, which is difficult at millimetre wave frequencies. Second, the reported frequency translator requires a sawtooth wave into the DC port of the MZMs. An MZM normally has a high DC port switching voltage and hence a high-amplitude sawtooth wave is needed to realise microwave signal frequency translation. Since the modulator DC port is occupied by the sawtooth wave, a bias controller cannot connect directly to the modulator DC port to avoid the modulator bias drift problem. A frequency translator with phase shifting ability was reported recently [13]. It requires an optical filter to remove an RF modulation sideband. The use of an optical filter limits the frequency translator lower operating frequency. Furthermore, this frequency translator is implemented by a dual-parallel Mach Zehnder modulator (DPMZM) in which the two sub-MZMs are biased at the peak and null point while the main MZM bias voltage is used to realise the phase shifting operation. It suffers from the modulator bias drift problem as other microwave photonic signal processors. A commercial DPMZM bias controller cannot be used to solve the problem because they are designed to lock the DPMZM bias point for realising single sideband suppressed carrier (SSB-SC) modulation.

This paper presents a new microwave photonic frequency translator structure to overcome the problems and limitations in the reported structures. The frequency translated microwave signal is produced by using Serrodyne phase modulation to frequency translate an optical carrier, which beats with the RF signal modulation sideband at the photodetector. This is different to that of the structure presented in [8]. The proposed frequency translator can realise frequency translation and phase shifting operation without the need of an optical filter. Additionally, off-the-shelf bias controllers can be incorporated to the proposed structure to obtain a long-term stable performance. The new microwave photonic frequency translator is analysed with results showing the effect caused by the phase imbalance of the coupler used in the frequency translator can be eliminated by designing the modulator bias voltages. Experimental results demonstrate frequency translation with

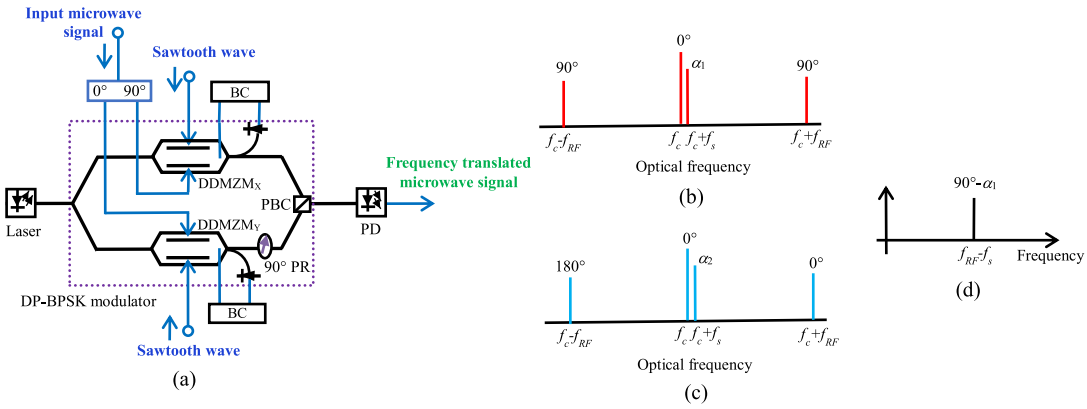

Fig. 1. (a) Schematic diagram of the proposed microwave photonic frequency translator based on a DP-BPSK modulator. DP-BPSK modulator output optical spectrum generated by (b) $\mathrm{DDMZM_X}$ and (c) $\mathrm{DDMZM_Y}$. (d) Frequency translator output electrical spectrum. f_c, f_{RF}, and f_s are the frequency of the optical carrier, the input microwave signal and the sawtooth wave respectively.

large spurious signal suppression, continuous 0° to 360° phase shift on the frequency translated microwave signal and a long-term stable performance.

2. Topology and Operation Principle

The structure of the proposed microwave photonic frequency translator is shown in Fig. 1(a). It has a simple laser-modulator-photodetector structure as a conventional fibre optic link [14]. The laser provides a continuous wave light with a frequency f_c to the system. The modulator is a dual-polarisation binary phase shift keying (DP-BPSK) dual-drive Mach Zehnder modulator. It consists of two dual-drive MZMs ($\mathrm{DDMZM_X}$ and $\mathrm{DDMZM_Y}$), a 90° polarisation rotator (PR) connected at $\mathrm{DDMZM_Y}$ output and a polarisation beam combiner (PBC). Each DDMZM has two RF ports and a DC port. A commercial DP-BPSK modulator (Fujitsu FTM7980EDA) also has a built-in photodiode after each DDMZM. The built-in photodiode allows the DDMZM output power to be monitored by a bias controller (BC). The DC bias voltage into the DDMZM is adjusted accordingly by the BC to avoid the modulator bias drift problem. A microwave signal, which needs to be frequency translated, passes through a 90° hybrid coupler. The two quadrature-phase microwave signals at the coupler outputs are injected into an RF port of $\mathrm{DDMZM_X}$ and $\mathrm{DDMZM_Y}$. Since a DDMZM can be modelled as two parallel-connected optical phase modulators, a microwave signal into an RF port of a DDMZM produces an optical carrier and two RF modulation sidebands at the frequencies of f_c and $f_c \pm f_{RF}$ where f_{RF} is the input microwave signal frequency. Similarly, two identical sawtooth waves with a frequency f_s are injected into the other RF port of $\mathrm{DDMZM_X}$ and $\mathrm{DDMZM_Y}$. This produces a frequency translated optical carrier at $f_c + f_s$ without power loss under an ideal situation [15]. The polarisation state of the optical signal at the output of $\mathrm{DDMZM_Y}$ is rotated by 90° via a 90° PR. Therefore, the DP-BPSK modulator output consists of two orthogonally polarised optical signals. The two optical signals do not interact with each other and are detected by a photodetector (PD).

Fig. 1(b) and 1(c) show the DP-BPSK modulator output optical spectrums in the two orthogonal polarisation states. Note from the figures that the two RF modulation sidebands from $\mathrm{DDMZM_X}$ have the same phase of 90° with respect to the optical carrier whereas the two RF modulation sidebands generated by $\mathrm{DDMZM_Y}$ are 180° out of phase. In both cases, the two sidebands beat with the optical carrier at the PD do not generate a frequency component at the original input microwave signal frequency f_{RF}. The phase of the frequency translated optical carrier from $\mathrm{DDMZM_X}$ and $\mathrm{DDMZM_Y}$ is $\alpha_1 = \pi V_{DC1}/V_{\pi,DC}$ and $\alpha_2 = \pi V_{DC2}/V_{\pi,DC}$ respectively. V_{DC1} and V_{DC2} are the DC bias voltage into $\mathrm{DDMZM_X}$ and $\mathrm{DDMZM_Y}$ respectively and $V_{\pi,DC}$ is the DDMZM

DC port switching voltage. Therefore, the phase of the frequency translated optical carriers at $f_c + f_s$ can be controlled by the DC bias voltages. The frequency translated optical carrier beat with the two sidebands at the PD generates microwave frequency components at $f_{RF} \pm f_s$. By designing the two DC bias voltages so that α_1-$\alpha_2 = 90°$, the frequency components at $f_{RF} + f_s$ generated by $DDMZM_X$ and $DDMZM_Y$ are 180° out of phase and hence they cancel each other. On the other hand, the frequency components at f_{RF}-f_s generated by $DDMZM_X$ and $DDMZM_Y$ are in phase. Hence under an ideal situation only the frequency component at f_{RF}-f_s is presence at the frequency translator output as shown in Fig. 1(d). This shows the input microwave signal at f_{RF} is translated to f_{RF}-f_s. The figure also shows the phase of the frequency translated microwave signal is 90°-α_1. This indicates that the frequency translated microwave signal phase can be tuned by controlling the modulator DC bias voltages, at the same time the condition α_1-$\alpha_2 = 90°$ needs to be maintained to eliminate the sideband at $f_{RF} + f_s$.

Commercial MZM bias controllers such as Plugtech MBC-MZM-01A MZM bias controllers can be used to control the two DDMZM bias voltages. They can lock the DDMZMs at any operating point in the modulator transfer function to maintain a stable performance while obtain the desired phase shift. It is worth noting that the amount of the microwave signal frequency translation is determined by the sawtooth wave frequency. Since only a small amount of frequency translation is needed for velocity deception, a low-cost dual-output waveform generator or single-output waveform generator followed by a power splitter can be used to produce two identical sawtooth waves.

3. Analysis and Simulation Results

The output of the DP-BPSK modulator based microwave photonic frequency translator is analysed in this section. We include the 90° hybrid coupler phase imbalance θ, the sawtooth wave fall time T_F and the DDMZM extinction ratio ε in the analysis to investigate how these non-ideal effects affect the frequency translator performance. When a microwave signal with a frequency f_{RF} and a sawtooth wave with a frequency f_s are injected into the DP-BPSK modulator as shown in Fig. 1(a), $DDMZM_X$ and $DDMZM_Y$ output electric field are given by

$$E_{DDMZM_X,out}(t) = \frac{1}{2\sqrt{2}} E_{in}\sqrt{t_{ff}} e^{j2\pi f_c t}\left[\sum_{n=-\infty}^{\infty} j^n J_n(\beta_{RF})\, e^{j(n2\pi f_{RF} t + n\theta)} + \gamma e^{j\alpha_1} \sum_{m=-\infty}^{\infty} a_m e^{j(m2\pi f_s t)}\right] \quad (1)$$

$$E_{DDMZM_Y,out}(t) = \frac{1}{2\sqrt{2}} E_{in}\sqrt{t_{ff}} e^{j2\pi f_c t}\left[\sum_{n=-\infty}^{\infty} J_n(\beta_{RF})\, e^{j(n2\pi f_{RF} t)} + \gamma e^{j\alpha_2} \sum_{m=-\infty}^{\infty} a_m e^{j(m2\pi f_s t)}\right] \quad (2)$$

where E_{in} is the electric field amplitude of the continuous wave light into the DP-BPSK modulator, t_{ff} is the insertion loss of each DDMZM, $J_n(x)$ is the Bessel function of nth order of the first kind, $\beta_{RF} = \pi V_{RF}/V_{\pi,RF}$ is the modulation index, V_{RF} is the voltage of the microwave signal into the RF port of the DDMZM, $V_{\pi,RF}$ is the DDMZM RF port switching voltage and $\gamma = (\varepsilon^{1/2}\text{-}1)/(\varepsilon^{1/2} + 1)$. The first and second term inside the square brackets in (1) and (2) show the amplitude and phase of the optical frequency components generated by microwave signal phase modulation and sawtooth wave phase modulation [15] respectively. Under an ideal situation ($T_F = 0$ s), a sawtooth wave with an amplitude equal to $2V_{\pi,RF}$ into an RF port of a DDMZM produces a frequency translated optical carrier at $f_c + f_s$ without power loss, i.e., $a_1 = 1$ and $a_m = 0$ where $m \neq 1$. However, in practice, a sawtooth wave has a finite fall time ($T_F \neq 0$ s) and the amplitude response of a DDMZM RF port is not constant with frequencies. Hence, in addition to the frequency translated optical carrier, unwanted optical frequency components at $f_c + mf_s$, where $-\infty < m < +\infty$ and $m \neq 1$, are generated. Their amplitude a_m is mainly dependent on the fall time to period ratio of the sawtooth wave [16].

The two orthogonally polarised optical signals with the electric field expressions given in (1) and (2) are detected by a PD. This produces a photocurrent, which can be expressed as

$$I(t) = \Re\left[\left|E_{DDMZM_X,out}(t)\right|^2 + \left|E_{DDMZM_Y,out}(t)\right|^2\right] \quad (3)$$

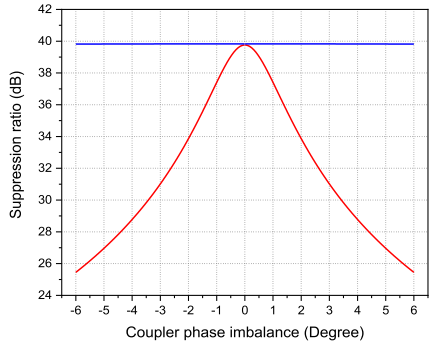

Fig. 2. Carrier (blue line) and sideband (red line) suppression ratio versus the 90° hybrid coupler phase imbalance.

where $\Re$ is the PD responsivity. The photocurrent at the frequency translated microwave signal frequency f_{RF}-f_s, the unwanted carrier frequency f_{RF} and the unwanted sideband frequency $f_{RF}+f_s$ can be obtained from (3). They are given by

$$I_{f_{RF}-f_s}(t) = \frac{1}{4}P_{in}t_{ff}\gamma J_1(\beta_{RF})\begin{bmatrix} a_1\sqrt{2-2\sin(\alpha_2-\alpha_1+\theta)}\cos(2\pi f_{RF}t-2\pi f_s t+\phi_A) \\ -a_{-1}\sqrt{2-2\sin(\alpha_1-\alpha_2+\theta)}\cos(2\pi f_{RF}t-2\pi f_s t+\phi_B)\end{bmatrix} \tag{4}$$

$$I_{f_{RF}}(t) = \frac{1}{2}P_{in}t_{ff}\gamma a_0 J_1(\beta_{RF})\sqrt{\sin^2\alpha_1+\sin^2\alpha_2-2\sin\alpha_1\sin\alpha_2\sin\theta}\sin(2\pi f_{RF}t+\phi_C) \tag{5}$$

$$I_{f_{RF}+f_s}(t) = \frac{1}{4}P_{in}t_{ff}\gamma J_1(\beta_{RF})\begin{bmatrix} -a_1\sqrt{2-2\sin(\alpha_1-\alpha_2+\theta)}\cos(2\pi f_{RF}t+2\pi f_s t+\phi_B) \\ +a_{-1}\sqrt{2-2\sin(\alpha_2-\alpha_1+\theta)}\cos(2\pi f_{RF}t+2\pi f_s t+\phi_A)\end{bmatrix} \tag{6}$$

where

$$\phi_A = \tan^{-1}\left(\frac{\sin(\alpha_1-\theta)+\cos\alpha_2}{\sin\alpha_2-\cos(\alpha_1-\theta)}\right) \tag{7}$$

$$\phi_B = \tan^{-1}\left(\frac{\cos\alpha_2-\sin(\alpha_1+\theta)}{-\sin\alpha_2-\cos(\alpha_1+\theta)}\right) \tag{8}$$

$$\phi_C = \tan^{-1}\left(\frac{\cos\theta\sin\alpha_1}{\sin\alpha_2-\sin\theta\sin\alpha_1}\right) \tag{9}$$

It can be seen from (4)-(9) that the amplitude and phase of the frequency translated microwave signal and the spurious signals are dependent on α_1, α_2 and θ. Fig. 2 shows the carrier suppression ratio $(I_{fRF\text{-}fs}/I_{fRF})^2$ and the sideband suppression ratio $(I_{fRF\text{-}fs}/I_{fRF+fs})^2$ as a function of the 90° hybrid coupler phase imbalance when the DC bias voltages are designed so that α_1-$\alpha_2 = 90°$ and the sawtooth wave has a fall time to period ratio of 1%. It can be seen from the figure that the carrier suppression ratio is independent to the coupler phase imbalance. When the 90° hybrid couple has no phase imbalance, the carrier suppression ratio and the sideband suppression ratio are the same, which are 39.8 dB. In order for the sideband suppression ratio to be above 34 dB, the 90° hybrid couple phase imbalance needs to be within ±2°.

An advantage of the proposed frequency translator is that the two DC bias voltages can be designed to have the relationship α_1-$\alpha_2 = 90°$-θ to compensate for the effect of the coupler phase imbalance on the carrier and sideband suppression ratio. Under this condition, the term (2-2sin(α_1-$\alpha_2+\theta$))$^{1/2}$ in (4) and (6) is eliminated. (4)-(6) become

$$I_{f_{RF}-f_s}(t) = \frac{1}{2}a_1P_{in}t_{ff}\gamma\cos\theta J_1(\beta_{RF})\sin(2\pi f_{RF}t-2\pi f_s t+90°-\alpha_1) \tag{10}$$

$$I_{f_{RF}}(t) = \frac{1}{2}a_0P_{in}t_{ff}\gamma\cos\theta J_1(\beta_{RF})\sin(2\pi f_{RF}t+90°-\alpha_1) \tag{11}$$

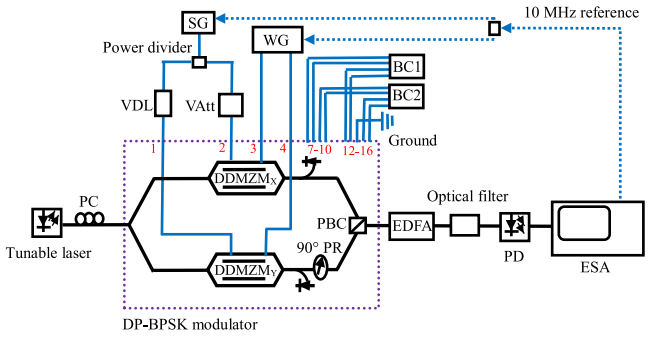

Fig. 3. Experimental setup of the DP-BPSK modulator based frequency translator. The DP-BPSK modulator pin numbers are labelled in red.

$$I_{f_{RF}+f_s}(t) = \frac{1}{2} a_{-1} P_{in} t_{ff} \gamma \cos\theta J_1(\beta_{RF}) \sin(2\pi f_{RF} t + 2\pi f_s t + 90^\circ - \alpha_1) \tag{12}$$

(10)-(12) show the amplitudes of all three photocurrents are proportional to cos θ. Thus, the frequency translated microwave signal to the spurious signal power ratios are independent to the 90° hybrid coupler phase imbalance θ. These power ratios are purely dependent on the coefficient a_m, which are in turn dependent on the sawtooth wave amplitude and fall time to period ratio. Simulation results in [15] show both $(a_1/a_{-1})^2$ and $(a_1/a_0)^2$ power ratios are larger than 40 dB for a sawtooth wave with a fall time to period ratio of below 1%, which can be achieved by commercial waveform generators. Hence over 40 dB spurious signal suppression can be obtained. Typical phase imbalance of a commercial 5-50 GHz bandwidth 90° hybrid coupler is ±5° [17]. A 5° phase imbalance in a 90° hybrid coupler causes only 0.03 dB reduction in the frequency translated microwave signal power according to (10). (10) also shows the phase of the frequency translated microwave signal is 90°-α_1. Therefore, shifting the phase of the frequency translated microwave signal and simultaneously having a large spurious suppression ratio can be realised by simply controlling the DDMZM DC bias voltages.

4. Experimental Results

An experiment was set up as shown in Fig. 3 to verify the frequency translation and the phase shifting operation in the proposed structure. The optical source was a tunable laser (Santec WSL-100), which generated a 1550 nm wavelength and 10 dBm optical power continuous wave light. A polarisation controller (PC) was used to align the light polarisation state to the slow axis before launching into a DP-BPSK modulator (Fujitsu FTM7980EDA). A microwave signal generator (SG) generated a 12 GHz microwave signal. As a 90° hybrid coupler was not available for experiments, a power divider followed by a variable delay line (VDL) and a variable attenuator (VAtt) were used to split the 12 GHz microwave signal into two with the same amplitude and quadrature phase. A dual-output waveform generator (WG) (Rigol DG4102) generated two identical sawtooth waves with a negative slope. The 12 GHz microwave signals and the sawtooth waves were applied to the RF ports of $\mathrm{DDMZM_X}$ and $\mathrm{DDMZM_Y}$. Two modulator bias controllers (Plugtech MBC-MZM-01A) were used to provide DC bias voltages to the two DDMZMs. An erbium-doped fibre amplifier (EDFA) and a 0.5 nm 3-dB bandwidth optical filter were connected to the DP-BPSK modulator output. They were used to compensate for the system loss to ensure a high average optical power of 10 dBm into the PD and to reduce the amplified spontaneous emission noise. The two orthogonally polarised output optical signals were detected by a PD (Discovery Semiconductor DSC30S-39), whose output was connected to an electrical signal analyser (ESA) to display the output electrical spectrum. The ESA, the SG and the WG were synchronised using a common 10 MHz reference signal.

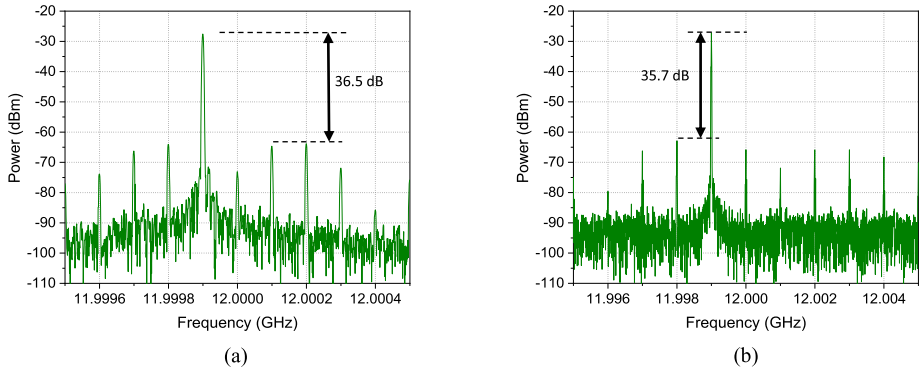

Fig. 4. DP-BPSK modulator based frequency translator output electrical spectrum for (a) 100 kHz and (b) 1 MHz sawtooth wave into the modulator. The input microwave signal frequency is 12 GHz.

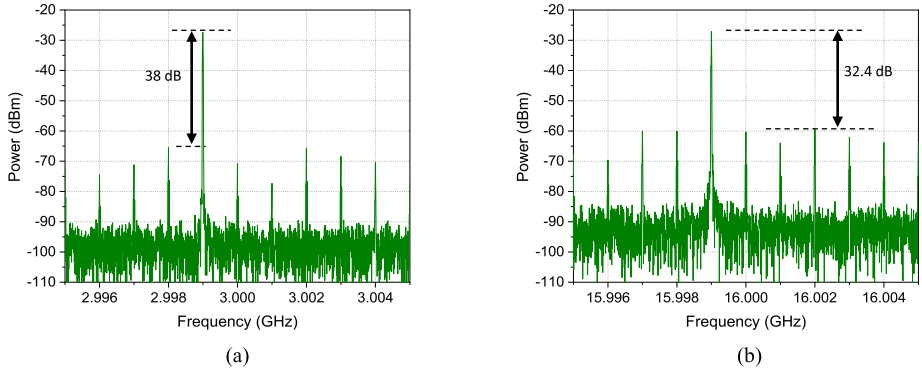

Fig. 5. DP-BPSK modulator based frequency translator output electrical spectrum for (a) 3 GHz and (b) 16 GHz microwave signal into the modulator. The sawtooth wave frequency is 1 MHz.

The fall time to period ratio of the sawtooth wave generated by the waveform generator was measured to be less than 0.7% when the sawtooth wave frequency is below 1 MHz. The ramp linearity of the sawtooth wave is less than 1% of the peak output. The amplitude of the sawtooth waves was set to be 5.3 V, which is around twice the DP-BPSK modulator RF port switching voltage. $\mathrm{DDMZM_X}$ and $\mathrm{DDMZM_Y}$ were biased at around the peak and quadrature point respectively to obtain the relationship α_1-$\alpha_2 = 90°$-θ. The frequency translator output electrical spectrum was measured on the ESA for different-frequency sawtooth waves into the modulator. Fig. 4(a) and 4(b) show the input microwave signal at 12 GHz is translated to 12 GHz $-$ 100 kHz and 12 GHz $-$ 1 MHz when the sawtooth wave frequency is 100 kHz and 1 MHz respectively. The spurious suppression ratio for 100 kHz and 1 MHz frequency translation is 36.5 dB and 35.7 dB respectively. The frequency translator spurious suppression ratio for an input sawtooth wave with different frequencies of between 100 kHz and 1 MHz was measured to be larger than 34 dB. This is more than 13 dB higher than the electronic frequency translator operating under the same input sawtooth wave frequency range [11]. It is also 14 dB higher than the commercial electronic frequency translators with a 0-500 kHz translation rate [12]. The frequency translator output electrical spectrum was also measured for different-frequency input microwave signals. Fig. 5(a) and 5(b) show the output electrical spectrum of the frequency translator when the input microwave signal frequency is 3 GHz and 16 GHz respectively, and the sawtooth wave frequency is fixed at 1 MHz. A 1 MHz frequency translation with over 32 dB spurious signal suppression can be seen from the figures. This demonstrates the frequency translator can be operated over a wide frequency range while having a large spurious suppression ratio.

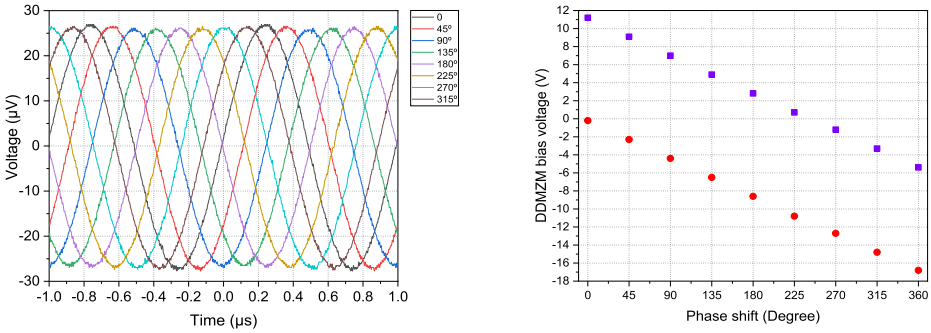

Fig. 6. (a) Waveforms of the frequency translated microwave signal after down conversion, for different $\mathrm{DDMZM_X}$ and $\mathrm{DDMZM_Y}$ DC bias voltages. (b) $\mathrm{DDMZM_X}$ (red circles) and $\mathrm{DDMZM_Y}$ (purple squares) DC bias voltage required to obtain different frequency translated microwave signal phase shifts.

The frequency translated microwave signal phase control ability in the proposed structure was investigated. The input microwave signal frequency was 12 GHz and the sawtooth wave frequency was 1 MHz. A 12 GHz $-$ 1 MHz frequency translated microwave signal was generated. Due to the lack of a high frequency oscilloscope, this frequency translated microwave signal was down converted to a 1 MHz signal via a frequency mixer (Minicircuits ZX05-24MH-S+). A 100 MHz bandwidth oscilloscope (Keysight DSO-X 2014A) was connected to the mixer output to observe the down converted signal phase shift. Fig. 6(a) shows the down converted signal waveforms displayed on the oscilloscope when different sets of DC bias voltages shown in Fig. 6(b) into the modulator. Since the phase shift in the down converted signal corresponds to the frequency translated microwave signal phase shift, the results in Fig. 6 demonstrate 0° to 360° frequency translated microwave signal phase shift can be obtained by controlling the DDMZM DC bias voltages. A linear relationship between the signal phase shift and the required DDMZM DC bias voltages can be seen in Fig. 6(b). The change in the DDMZM DC bias voltage required to obtain a 180° phase shift is 8.4 V, which is the same as $\mathrm{DDMZM_X}$ and $\mathrm{DDMZM_Y}$ DC port switching voltage. The difference between the two DDMZM DC bias voltages needs to be maintained at around 11.4 V to obtain a large spurious suppression ratio as shown in the frequency translator output electrical spectrum in Fig. 7, during the phase shifting operation. This verifies the bias condition α_1-$\alpha_2 =$ 90°-θ after considering that there is -1 V shift in $\mathrm{DDMZM_X}$ transfer function compared to $\mathrm{DDMZM_Y}$. Fig. 7 shows there is less than 0.4 dB variation in the frequency translated microwave signal power when changing the DDMZM DC bias voltages to realise frequency translated microwave signal phase shift. The experimental results in Fig. 4, 5 and 7 show the output of the frequency translator consists of the frequency translated microwave signal and a number of spurious signals. These spurious signals are mainly due to the non-ideal sawtooth wave into the DP-BPSK modulator, which can be suppressed by using a sawtooth wave with a smaller fall time to period ratio. They can also be suppressed by improving the phase imbalance of the microwave signal and the sawtooth wave into the two DDMZMs inside the DP-BPSK modulator. Nevertheless, the spurious signals shown in Fig. 4, 5 and 7 are more than 30 dB, i.e., more than 1000 times, below the frequency translated microwave signal. Hence, they have little effect on the frequency translated microwave signal.

The frequency translator spurious suppression ratio was measured for different input microwave signal powers. Fig. 8(a) shows the power ratio of the 12 GHz $-$ 1 MHz frequency translated microwave signal to the largest-amplitude spurious signal is over 34.5 dB when the power of the microwave signal into the RF port of the DDMZM was changed from -19.3 dBm to 1.6 dBm. This 20.9 dB change in the input microwave signal power corresponds to the modulation index changes from 0.04 to 0.4. This indicates that the frequency translator can handle different input microwave signal powers while having a large spurious suppression ratio. The frequency translator spurious suppression ratio was recorded every 5 minutes. Fig. 8(b) shows a large spurious suppression ratio

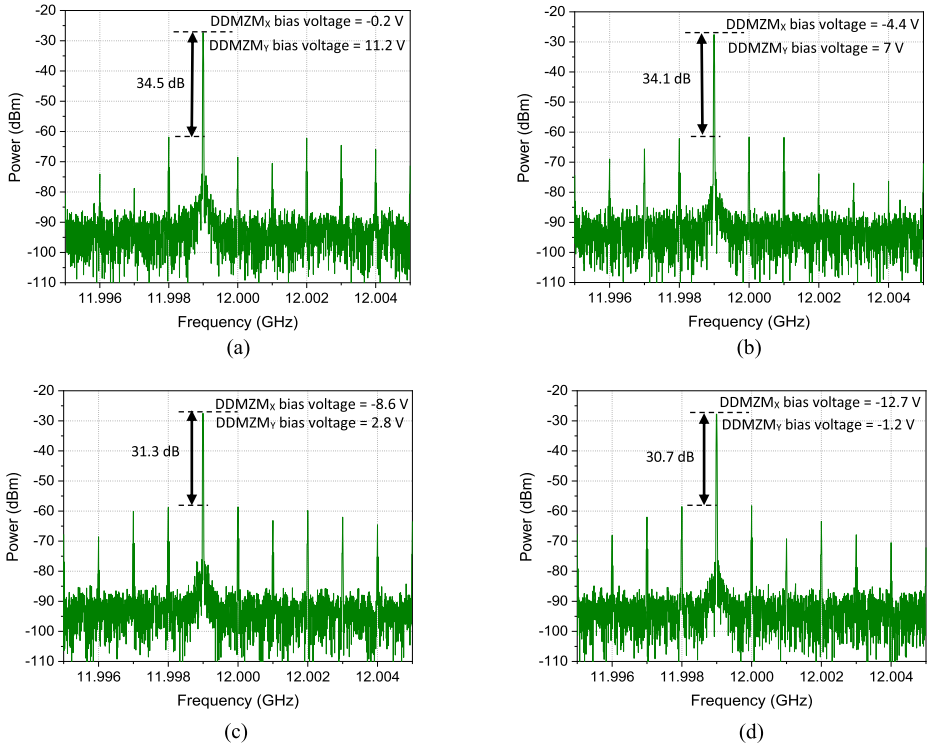

Fig. 7. Frequency translator output electrical spectrums when $DDMZM_X$ and $DDMZM_Y$ DC bias voltages are adjusted to obtain (a) 0°, (b) 90°, (c) 180°, and (d) 270° phase shift.

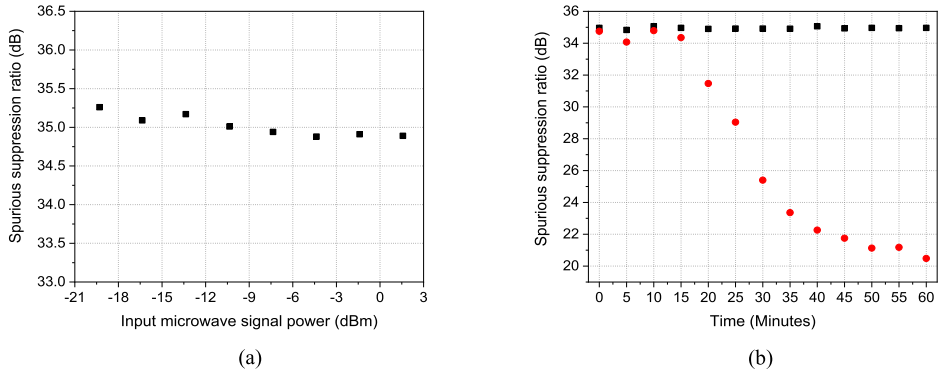

Fig. 8. (a) Measured spurious suppression ratio versus the power of the microwave signal into the DP-BPSK modulator. (b) Measured spurious suppression ratio when using modulator bias controllers (black squares) and DC power suppliers (red circles) to provide DC bias voltages to the DDMZMs.

of around 35 dB can be maintained over an hour when modulator bias controllers were used to lock the DDMZM operating points. On the other hand, the spurious suppression ratio continuously reduces after 15 minutes when simply using DC power supplies to provide DC bias voltages to the DDMZMs. This demonstrates another advantage of the DP-BPSK modulator based frequency translator that is the structure enables off-the-shelf bias controllers to be used to maintain a large spurious suppression ratio performance. Since the bias controllers (Plugtech MBC-MZM-01A) used in the experiment can lock the DDMZMs at any point in the modulator transfer function, experimental results also demonstrated the phase of the frequency translated microwave signal remained the same over a long period of time after adjusting the DDMZM DC bias voltages via

the bias controllers to realise the phase shifting operation. The new DP-BPSK modulator based frequency translator has 10 dB improvement in the spurious suppression ratio compared to the commercial electronic frequency translators, which have a typical carrier and sideband suppression of 25 dB and 20 dB respectively [12]. It also has a wide operating frequency range, which is only limited by the bandwidth of the 90° hybrid coupler used in the setup. A 6-67 GHz bandwidth 90° hybrid coupler is commercially available.

5. Conclusion

A new microwave photonic frequency and phase shifter has been presented. It has the ability to simultaneously shift the frequency and phase of a microwave signal for deception jamming. It generates a frequency translated microwave signal with large spurious signal suppression, which cannot be achieved by conventional frequency mixers. Shifting the frequency translated microwave signal phase and simultaneously eliminating the effect of the phase imbalance of the 90° hybrid coupler used in the structure are realised by controlling the modulator DC bias voltages. The frequency translator also has the advantage that commercial modulator bias controllers can be used to avoid the modulator bias drift problem, which is presence in all microwave photonic signal processors that involve optical modulators. Experimental results show the frequency translator is capable to provide different amount of microwave signal frequency translation suitable for velocity deception. A wide operating frequency range of 3 to 16 GHz has been demonstrated, which overcomes the bandwidth limitation in electronic frequency translators. Results also demonstrate a continuous 0° to 360° phase shift on the frequency translated microwave signal with less than 0.4 dB power variation. Using modulator bias controllers in the proposed structure to maintain a large spurious suppression ratio of around 35 dB over an hour has also been demonstrated.

References

[1] S. Mazumder and C. Isham, "Frequency translation by phase shifting," in *Appl. Microw. Wireless*, 1995, pp. 59–71.
[2] W. W. Shrader and V. Gregers-Hansen, "MTI radar," in *Radar Handbook* (2nd ed.) Chapter 15, New York, NY, USA: McGraw-Hill, 1990.
[3] Q. Feng, H. Xu, Z. Wu, and W. Liu, "Deceptive jamming detection for SAR based on cross-track interferometry," *Sensors (Basel)*, vol. 18, no. 7, 2018, Art. no. 2265.
[4] J. Zhang, E. H. W. Chan, X. Wang, X. Feng, and B. Guan, "Broadband microwave photonic sub harmonic downconverter with phase shifting ability," *IEEE Photon. J.*, vol. 9, no. 3, 2017, Art. no. 5501910.
[5] T. Li, E. H. W. Chan, X. Wang, X. Feng, B. Guan, and J. Yao, "Broadband photonic microwave signal processor with frequency up/down conversion and phase shifting capability," *IEEE Photon. J.*, vol. 10, no. 1, 2018, Art. no. 5500112.
[6] T. Jiang, R. Wu, S. Yu, D. Wang, and W. Gu, "Microwave photonic phase-tunable mixer," *Opt. Exp.*, vol. 25, no. 4, pp. 4519–4527, 2017.
[7] F. Yang *et al.*, "A microwave photonic phase-tunable mixer with local oscillator frequency doubling," *Opt. Commun.*, vol. 438, pp. 141–146, 2019.
[8] S. T. Winnall, A. C. Lindsay, and G. A. Knight, "A wide-band microwave photonic phase and frequency shifter," *IEEE Trans. Microw. Theory Techn.*, vol. 45, no. 6, pp. 1003–1006, 1997.
[9] K. J. Williams, "Electro-optical broadband microwave frequency shifter," U.S. Patent 6043926, 2000.
[10] C. S. McDermitt and F. Bucholtz, "RF frequency shifting via optically switched dual-channel PZT fiber stretchers," *IEEE Trans. Microw. Theory Techn.*, vol. 53, no. 12, pp. 3782–3787, 2005.
[11] W. Tang and H. Kim, "Low spurious, broadband frequency translator using left-handed nonlinear transmission line," *IEEE Microw. Wireless Compon. Lett.*, vol. 19, no. 4, pp. 221–223, 2009.
[12] G. T. Microwave frequency translators, [Online]. Available: http://gtmicrowave.com/, 2021
[13] C. Huang and E. H. W. Chan, "Photonics-based serrodyne microwave frequency translator with large spurious suppression and phase shifting capability," *J. Lightw. Technol.*, vol. 39, no. 7, pp. 2052–2058, 2021.
[14] C. H. Cox, III, G. E. Betts, and L. M. Johnson, "An analytic and experimental comparison of direct and external modulation in analog fiber-optic links," *IEEE Trans. Microw. Theory Techn.*, vol. 38, no. 5, pp. 501–509, 1990.
[15] L. M. Johnson and C. H. Cox, "Serrodyne optical frequency translation with high sideband suppression," *J. Lightw. Technol.*, vol. 6, no. 1, pp. 109–112, 1988.
[16] C. Laskoskie, H. Hung, T. El-Wailly, and C. L. Chang, "Ti-LiNbO$_3$ waveguide serrodyne modulator with ultrahigh sideband suppression for fiber optic gyroscopes," *J. Lightw. Technol.*, vol. 7, no. 4, pp. 600–606, 1989.
[17] Marki Microwave QH-0550 3 dB quadrature (90 degree) hybrid coupler, [Online]. Available: https://www.markimicrowave.com/hybrids/qh-0550.aspx, 2021